CAVITATION IN HIGH ENERGY PUMPS— DETECTION AND ASSESSMENT OF DAMAGE POTENTIAL

by
Donald P. Sloteman
Manager, Advanced Technology
Curtiss-Wright, Electro-Mechanical Corporation
Phillipsburg, New Jersey

Donald P. Sloteman is Manager of Advanced Technology for Curtiss Wright, Electro-Mechanical Corporation's Engineered Pump Division, in Phillipsburg, New Jersey. He is responsible for managing the development and application of technology to pumps for service on U.S. Navy ships. He joined Ingersoll-Rand's Corporate Research Center as a project engineer. Mr. Sloteman worked for Ingersoll-Dresser Pump Company and Flowserve Pump Division prior to joining Curtiss Wright. He has held positions of Senior Project Engineer, Program Manager, and Manager, Pump R&D prior to his present position. In addition to his management of technology assignment, he also manages the Alexey J. Stepanoff Memorial Hydraulic Laboratory, in Phillipsburg, New Jersey.

Mr. Sloteman received his B.S. degree (Mechanical Engineering) from Drexel University and his M.S. degree (Engineering, Executive Engineering) from the University of Pennsylvania. He is a member of ASME.

ABSTRACT

Cavitation in centrifugal pumps is one of the fundamental factors that affect performance, operability, reliability, and life. Every major manufacturer of engineered, high-energy, centrifugal pumps has addressed these issues. As a result, industry, academia, pump users, and independent agents have engaged in technology development efforts over the past quarter century that have contributed to understanding, predictive tools, new erosion resistant materials, and advanced fluid designs that improve the performance, operability, reliability, and life of high-energy pumping machines. The technology development continues as new generations of pump engineers confront cavitation problems; new methods are developed to detect cavitation and assess damage potential. In addition, advanced computational prediction tools are evolving to allow prediction of the size and extent of cavitation vapor in the impeller. This paper discusses recent development and application of such tools and discusses possible future development of detection and assessment tools.

INTRODUCTION

The formation and consequences of cavitation in centrifugal pumps are one of the fundamental issues affecting pump operation. All users are familiar with the deterioration in developed head as suction pressure is reduced to where cavitation vapor is present to a sufficient degree to block the impeller passages and limit head development. A photo of such behavior is presented in Figure 1. An additional concern is when the intensity of the cavitation return to the liquid phase is increased due to the higher relative velocities on the impeller that come about from higher tip speeds. It is known that the tip speed increases with higher energy level. The fundamental relationship between a cavitation vapor bubble and the pressure generated upon its collapse was discussed by Rayleigh (1917). The energy release and pressure wave formed by the change of phase from vapor to liquid are the key factors in cavitation erosion damage (the other being a corrosion factor caused by the high local temperature increase accompanying the change of phase). Thiruvengadam (1973) developed a relationship that coupled the cavitation bubble dynamics with materials, relative velocity, and extent of the cavitation vapor with erosion damage on an impeller. What was clear from the study of dynamics of cavitation was that the performance net positive suction head (NPSH) varied with the well-known similarity laws and the damage rate increased far faster as tip speeds increased. Also shown in Figure 1 is an impeller blade that has suffered cavitation erosion due to vapor collapse on both the surface of the blade and in the fillet area where the blade joins the hub surface.

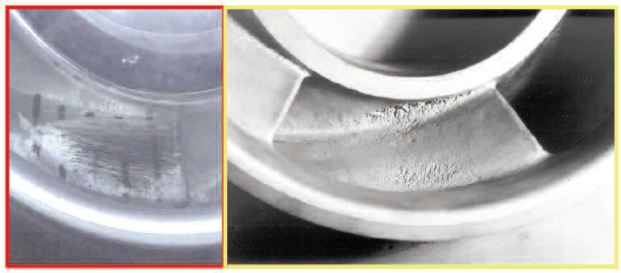

Figure 1. Cavitation and its Effects on a Centrifugal Pump Impeller. (A consequence of cavitation in high-energy pumps, shown in the left view, is the erosion pattern seen in the right hand view.)

As high-energy pumps, typified by multistage boiler feed pumps used in fossil fueled steam plants, became larger in the 1970s to satisfy higher capacities, pump designers relied upon the affinity laws, applied to lower energy hydraulic models, to establish the impeller designs for these larger machines. While this produced designs of known overall performance, the plants often did not provide enough NPSH for the pump to avoid operation with

Table of Contents

significant cavitation of the type pictured in Figure 1. At the higher tip speeds needed to support the higher heads and pressures of the supercritical steam cycles used in the larger plants, suction-impeller erosion rates were found to be far greater than on lower energy machines of similar hydraulic design. Also, many of the large plants were called upon to cycle loads that caused the impeller to operate away from its intended design flow coefficient (ϕ). One of the earliest studies documenting these problems is from Makay and Szamody (1978). Here, power station outages due to feed pump problems were cataloged and analyzed. Cavitation erosion of suction impellers was identified as a major problem.

Through the 1980s pump manufacturers from North America and Europe began to more actively address the cavitation erosion problem (Florjancic, 1980; Cooper and Antunes, 1982; Dernedde and Steck, 1982; Aisawa and Schiavello, 1986; and Gopalakrishnan, 1985). This reported work sought to align the observed field observations with design factors coupled with a basic knowledge of the physics involved. In the case of Gopalakrishnan (1985), he compiled technology from multiple sources and discussed critical aspects of cavitation formation, detection, and damage quantification known to that time. The experimentally based topics he covered included:

- Cavitation potential based on visual inception.
- Erosion potential based on paint removal.
- Erosion potential based on cavity length.
- Broadband acoustic determination of erosion potential.
- Erosion potential based on spike energy above a threshold noise level.
- Radioactive methods of erosion rate.
- Erosion from empirical methods based on design.

As will be seen, this vision of the technology development required to master the cavitation erosion problem, would form a basis for work performed (mostly in the industrial R&D environment) for the next 20 years.

A comprehensive understanding of the factors (more heavily on operation than design) that influenced the erosion problem came from Guelich (1989). In this study, Guelich compiled a report that relied on applying the existing knowledge of the physics of cavitation with field and laboratory testing and methods to quantify the erosion potential for an impeller design. However complete Guelich's work was regarding conventionally designed impellers, it did not explore alternate design approaches that would extend the life of suction impellers beyond the state-of-the-art.

Through the 1990s, the pump industry worked to improve the designs of high-energy, suction stage impellers. Nearly every manufacturer was active to some degree in this pursuit, many using flow visualization. Papers reporting this work include: Schiavello and Prescott (1991); Cooper, et al. (1991a); Cooper, et al. (1991b); Bolleter, et al. (1991); Sloteman, et al. (1995); and Hergt, et al. (1996). The fruition of much of this work was found in successful upgraded retrofits to high-energy feed pump suction stages such as described in Sloteman, et al. (2004). Sloteman's work utilized flow visualization testing that allowed for optimization and evaluation via visual means. Increased suction stage life was achieved through redesign of the impeller with no appreciable deterioration in overall pump performance.

However, without benefit of flow visualization testing of the exact hydraulic design, other means for characterizing and redesign were required. The listing of experimental methods in Gopalakrishnan (1985) provides a reference for development of diagnostic and analytical methods that would be useful in dealing with cavitation erosion problems. The only method not discussed by Gopalakrishnan is the use of computational fluid dynamics (CFD) to evaluate the two-phase behavior of a centrifugal impeller. It was not until the turn of the century that practical CFD tools, using Reynolds averaged Navier Stokes (RANS) solvers, were made accessible to pump designers. With this tool the designer had a means of assessing cavitation formation and cavitation caused performance losses, but not a definitive model for erosion rate.

This paper will describe recent development efforts directed at improving one pump manufacturer's understanding the cavitation problem. Its topics include:

- CFD based cavitation formation prediction.
- Cavitation erosion potential based on cavity length.
- Cavitation detection and damage potential assessment.

Experimental Test Capability

One experimental laboratory used to study cavitation in pumping machinery was a hydraulic laboratory in Phillipsburg, New Jersey. This facility is equipped to perform cavitation testing that includes flow visualization of full-size models of high-energy pump suction stages, at reduced speed over a range of NPSH and flow rates. A typical test pump is shown in Figure 2. It is equipped to view the impeller through a transparent interface built into the suction inlet. The impeller and diffuser are identical to actual production pump designs. Use of a test pump such as this allows the experimenter to generate detailed mapping of cavitation formation and performance over a range of flows and NPSH values. The cavitation shown in Figure 1 came from this test pump. It also allows for measurement of the mechanical and fluid response to cavitation behavior.

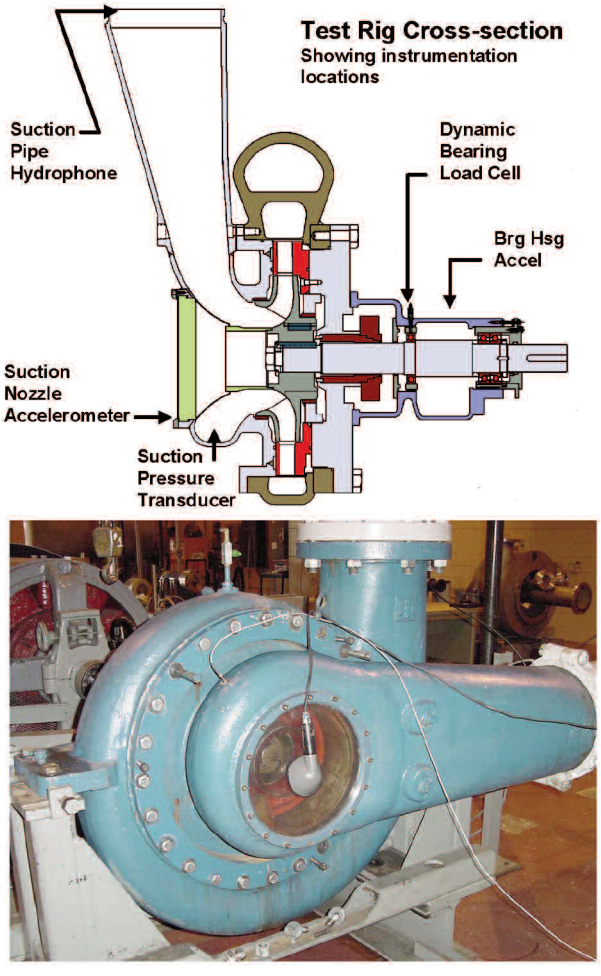

Figure 2. Flow Visualization Test Pump. (A full-size model of a production boiler feed pump suction stage is installed in a bearing housing/stuffing box/volute package along with sufficient instrumentation and transparent window to characterize the cavitating performance of the impeller.)

This test pump was also equipped with a complement of sensors capable of measuring dynamic pressure in the fluid, bearing forces, casing vibration, and airborne noise. As will be seen in this paper, the availability of flow visualization results from a model pump such as this coupled with a suitable erosion rate correlation makes it possible to fairly accurately predict the cavitation life of a suction impeller. However, absent the availability of such flow visualization or cavity length information, other means are needed to assess the damage potential.

Erosion Rate Based on Cavity Length

One of the fundamental approaches of calculating expected cavitation life of an impeller is to use sheet cavity length on the blade surface (suction side or pressure side). A logical development from the work of Thiruvengadam (1973) was the correlation of damage to actual impellers with sheet cavitation length by Guelich (1989). Guelich accounted for most of the factors that influence erosion, at least for the sheet cavity form of cavitation. For pumps operating under suction recirculation the relationship may not be relevant as a well-defined cavity length is not present.

The use of the relationship to predict cavitation life is dependent upon knowing what the cavity length is. Guelich (1989) correlated damaged impellers from which he could deduce the cavity length (he fairly assumed that the maximum damage location was where the sheet cavity closed, which he then confirmed with flow visualization).

The expression of the Guelich correlation, reformulated, is found in Cooper (2000) and is in Equation (1) below.

$$MDPR = \frac{\left[C \times \left(L_{cav} / 10\right)^n \times \left(\tau_A - \phi_e^2\right) \times U_e^6 \times \rho_L^3 \times A\right]}{\left[8 \times F_{mat} \times TS^2\right]} \quad \textbf{(1)}$$

This relationship calculates an erosion rate for either:

1. Suction surface sheet cavity—C = 8.28 E-06, n = 2.83.

2. Pressure surface sheet cavity—C = 396 E-06, n = 2.6.

The cavitation number τ is defined in Equation (2) as:

$$\tau = NPSH / \left(U_e^2 / 2g\right) \quad \textbf{(2)}$$

In Cooper (2000) a means of estimating the cavity length of an impeller based on the relation of operating NPSH to that impeller's NPSH3% value and the ideal inception NPSH was defined. While this is inferior to observing the exact cavity length, it does represent a method for using readily available impeller performance information and converting it into a cavitation life.

The cavity length approach was more appealing than methods based on empiricism such as Vlaming (1989). Here field damage history (including off-design operation) was coupled with basic impeller geometric dimensions and operating conditions to predict life. Methods based mainly on empiricism lacked the connection with the detailed impeller blade geometry that is the primary determinant of cavitation vapor behavior.

Sloteman, et al. (2004), used flow visualization tests to correlate the life of a suction stage impeller with cavity length. They also observed that cavity length varied with the circumferential location of the blade. For pumps that have suction impellers fed by a right angle suction inlet (as is the case for all between-bearing, high-energy pumps) some distortion of the inlet flow field is created. Regions of positive and negative prerotation are generated by the flow split around the shaft. Also, circumferential variations in mass flow can occur. The severity of the variations depends upon the specific design of the inlet. Those circumferential variations that exist will deliver different inlet flow conditions to the impeller and affect the formation of cavitation as well as the separation and suction recirculation characteristics associated with off-design flow rates. The influence of circumferential flow field variation on cavity length is seen in Figure 3. This full, 360 degree view of a high-energy pump suction stage eye reveals shorter cavity length in the top position (region of positive prerotation) and longer cavity length at the bottom position (region of negative prerotation).

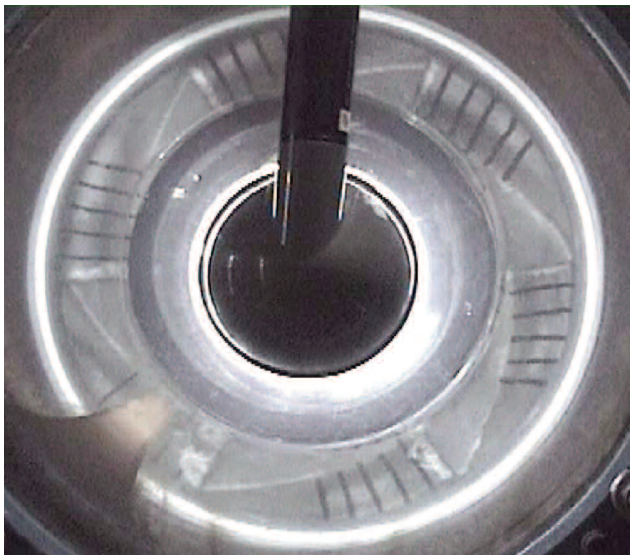

Figure 3. Example of Laboratory Based Flow Visualization. (This full 360-degree view of a cavitating test impeller shows the early stages of sheet cavitation. Circumferential distortion of the flow produces the varying cavity lengths. The impeller is operating at 100 percent of its design flow and at a cavitation number of 0.99.)

A calculation of erosion rates (from Guelich, 1989) for this impeller (having a known operating life) at the plant flow and NPSH condition (τ = 0.41) can be made that accounts for the varying cavity lengths. This impeller operated much of its life at base load. The inlet was divided into quadrants in order to capture the flow variations entering the impeller eye. The base load cavity length observed in each of four quadrants of the impeller contributed equally to the life. The impeller blade spent ¼ of its life in each of the quadrants. Table 1 lists the cavity lengths and averaged life of the impeller for each quadrant for both complete perforation of the blade and also a 75 percent depth. Also shown is cavitation life using the basic Cooper (2000) estimate of cavity length.

Table 1. Comparison of Life using the Guelich (1989) Life Equation.

Position	Cav Length inch	φ local	MDPR mm/hr	hrs/inch	Life-perforation hrs	Life-75% hrs
Visual Determination of Length						
0	2	0.202	0.00150	16903	6423	4817
90	2.3	0.2	0.00211	12033	4573	3429
180	1.3	0.268	0.00031	83124	31587	23690
270	1.75	0.195	0.00105	24113	9163	6872
				Impeller Life - Sum/4	**12936**	**9702**
Pump Handbook Length Calc						
0	2	0.2	0.00151	16778	6376	4782
90	2	0.2	0.00151	16778	6376	4782
180	2	0.2	0.00151	16778	6376	4782
270	2	0.2	0.00151	16778	6376	4782
				Impeller Life - Sum/4	**6376**	**4782**

The field life of this impeller ranged from 12,000 to 16,000 hours. The calculated average of 13,000 hours fits within this experience range significantly better than the uniform cavity length prediction (6400 hours). It appears that when nonuniform cavity lengths are present, assuming a uniform, average length will under predict the expected life. The ability to produce positive prerotation

over a substantial portion of the inlet is also beneficial to reducing cavity length and increase life (although it is known that this will also reduce the developed head of the stage also).

Many factors influence suction inlet design and the resulting degree of circumferential variations imposed on the flow field entering the impeller. It is clear that such variation needs to be accounted for in order to improve the accuracy of predicted cavitation life. The combination of experimental flow visualization of a suction stage design (including the impeller and suction inlet approach) with the Guelich (1989) life relationship produces reasonable predictions of field life, at least for pumps that operate mostly around the design point condition. However, a less costly means of determining the circumferential cavity length function for the impeller is needed. This method would be able to predict the cavity length as a function of the inlet flow field produced by the suction inlet.

Computational Fluid Dynamics

The tool that has come to maturity for fluid machinery design is modern, commercially available, computational fluid dynamics codes. These codes utilize Reynolds averaged Navier Stokes solvers to calculate solutions to flow problems that capture much of the inertial and viscous behaviors of the fluid. While more sophisticated, high-end CFD tools are available, the practical RANS solver can be used by the pump designer to optimize designs before they transition to costly hardware.

More recently, these RANS codes have been adapted to include multiphase modeling as well. With this capability, the designer can evaluate the suction performance of the machine and also the extent of cavitation vapor present on the blades. At present, the two-phase modeling has been applied to flow rates around the design condition. The unsteady nature of off-design flow rates dramatically complicates the steady-state CFD solution and unless a fully transient solution is pursued (a computationally intensive, time consuming, and costly approach) CFD cannot be readily applied. Sloteman, et al. (2004), summarize the evolution of this software tool and its application to pump design.

Multiphase CFD was used to analyze the high-energy impeller described by Sloteman, et al (2004), and discussed in the previous section on cavitation life. The RANS code was used to calculate the flow through the right angle, suction inlet approach to the impeller. The resulting flow field (divided into quadrants) was used as inlet boundary conditions for a two-phase impeller solution. An example of the result for one quadrant is shown in Figure 4. The CFD solution is shown at the right for the quadrant that produced approximately zero prerotation. Good correlation with the flow visualization result is seen. The two-phase CFD approach is also suitable for predicting the classic head versus NPSH characteristic for constant flow. To do this, multiple CFD solutions are required with incremental decreases in inlet pressure applied at the inlet boundary. For this example, an average inlet flow field was used (not the circumferentially varying profile known to exist). The result is shown in Figure 5 and shows good correlation with experimental test results.

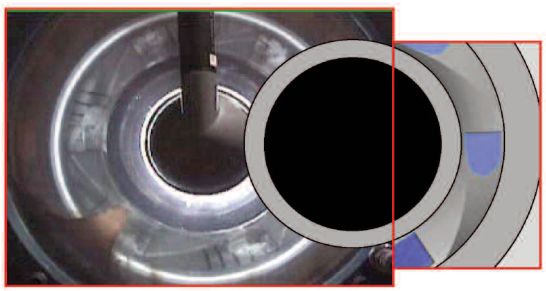

Figure 4. Cavitation Formation Prediction Using CFD. (The computed cavity length shown at right in the region of the inlet that produces zero preswirl, correlates with flow visualization results.)

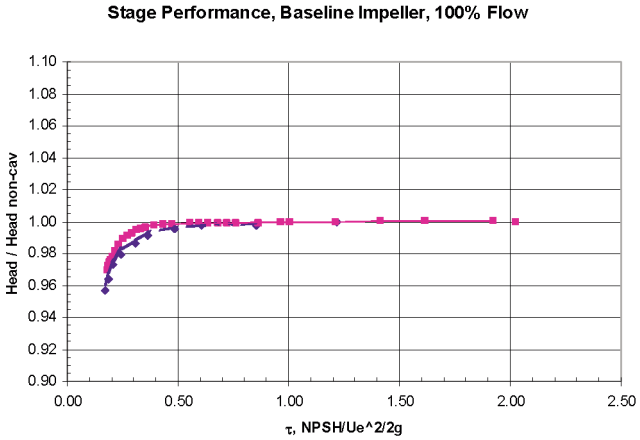

Figure 5. Suction Performance Prediction Versus Test Data for Suction Impeller. (The CFD calculation is based on a zero inlet prewhirl condition [a condition that usually occurs at only one circumferential location in a radial inlet suction bay]. In spite of this, good correlation with test data is observed.)

The CFD effort to analyze in detail each of the four quadrants of the suction inlet produced the mosaic of cavity lengths shown in Figure 6. Flow enters the suction bay from the position labeled 180 degrees. The inlet pressure applied at the suction inlet (and losses accounted for as the flow reached each of the four quadrants) replicated the nondimensional cavitation number present at the plant. The resulting circumferential variation in cavity length was very similar to that found on test (refer to Figure 4). One area needing explanation regards the 90-degree location, or the bottom position in Figure 4. In this region of negative prerotation, fluctuating cavity length was observed that accounts for the apparent shortness of the cavity in the Figure 4 photo. The instant the digital image was captured reflected a momentary shorter cavity length.

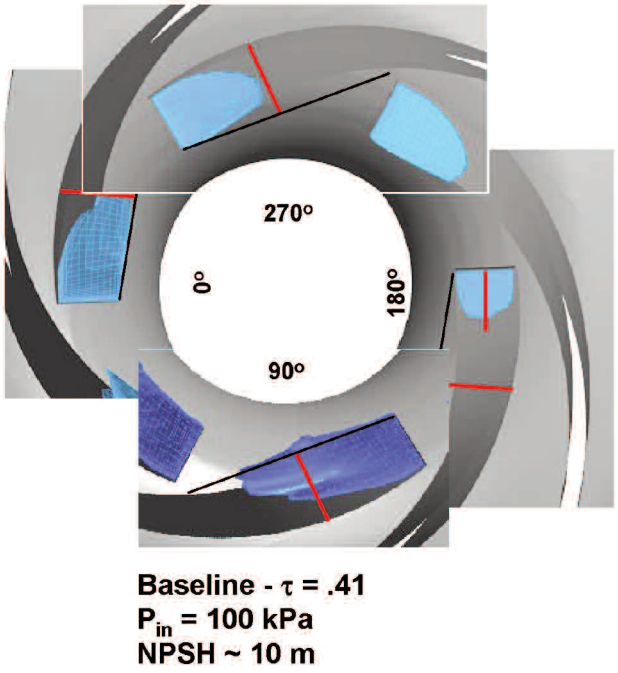

Figure 6. Computed Circumferential Variation of Sheet Cavitation Due to Suction Inlet Design. (Circumferential variation in prerotation and mass flow result in significant difference in sheet cavity length.)

Also accounted for in the cavity length variations are circumferential differences in mass flow through each quadrant.

The column in Table 1 labeled ϕ_{local}, shows the CFD computed differences in flow coefficient from quadrant to quadrant. It is the combined influence of mass flow and prerotation differences from quadrant to quadrant that cause the variations in cavity lengths.

The multiphase CFD code used for this analysis relied on a model of the vapor phase behavior that is referred to as the volume of fluid (VOF) approach. This approach is described in more detail by Sloteman, et al. (2004). The result is that the solution provides an approximation of the volume of vapor (i.e., cavitation) at each node of the solution. In order to accurately predict the extent of the cavitation vapor on the blade, some knowledge of how to interpret the solution (that provides a percentage of vapor present at each node) is required. Use of the flow visualization results is made to determine the percentage of calculated vapor that corresponds to the visual extent of the cavitation on the blade. Having circumferentially varying cavity length increases the number of conditions available for the correlation.

The plot in Figure 7 shows cavity lengths from flow visualization, the Cooper (2000) method (both used for Table 1 life predictions), and for vapor fractions of 10 percent, 12.5 percent, and 15 percent. The >12.5 percent vapor fraction defines the extent of nodes in the solution that are considered to be vapor based on the visual results.

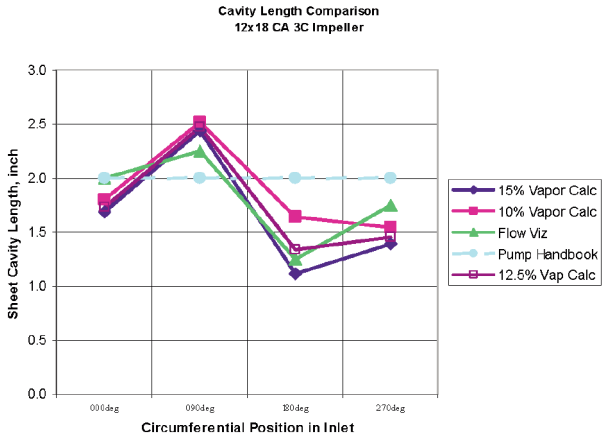

Figure 7. Computed Circumferential Variation of Sheet Cavitation Due to Suction Inlet Design. (Circumferential variation in prerotation and mass flow result in significant difference in sheet cavity length.)

When the circumferentially varying cavity lengths are used with the erosion prediction relationship, Table 1 can be generated. Table 2 shows the impeller life that would be predicted for the subject pump based only on CFD prediction of inlet flow field and cavitation formation in the pump impeller. The multiple vapor fractions are shown for reference, however the 12.5 percent value still provides the best correlation with visual results and actual field experience.

Table 2. Comparison of Cavitation Life from CFD Results.

Position	Cav Length inch	φ local	MDPR mm/hr	hrs/inch	Life-perforation hrs	Life-75% hrs
CFD Solutions - 10% Vapor						
0	1.8	0.202	0.00111	22803	8665	6499
90	2.5	0.2	0.00291	8735	3319	2489
180	1.6	0.268	0.00067	38171	14505	10879
270	1.5	0.195	0.00074	34414	13077	9808
				Impeller Life - Sum/4	**9892**	**7419**
CFD Solutions - 12.5% Vapor						
0	1.7	0.202	0.00100	25386	9647	7235
90	2.5	0.2	0.00276	9215	3502	2626
180	1.3	0.268	0.00037	68482	26023	19517
270	1.5	0.195	0.00063	40525	15399	11550
				Impeller Life - Sum/4	**13643**	**10232**
CFD Solutions - 15% Vapor						
0	1.7	0.202	0.00093	27416	10418	7813
90	2.4	0.2	0.00264	9604	3649	2737
180	1.1	0.268	0.00022	115686	43961	32970
270	1.4	0.195	0.00056	45597	17327	12995
				Impeller Life - Sum/4	**18839**	**14129**

The use of flow visualization or two-phase CFD results to define cavity lengths, coupled with the life equation of Guelich (1989) is suitable for predicting the life of suction impellers operating at or near the design condition (where sheet cavitation exists). However, when pumps are in the field or on the test stand exact knowledge of cavity lengths may not be obtainable. The estimates of Cooper (2000) are just that, estimates and predict shorter life than would be expected (refer to Table 1). A detection tool that can be applied, in real time, to pumps where flow visualization is impractical or if lack of detailed knowledge of the design prevents CFD analysis, would be useful in assessing the damage potential of high-energy pumps.

Detection and Assessment

The availability of a noninvasive means for detecting and assessing the damage potential of cavitation in any pump, operating at any condition, would be useful in identifying cavitation problems and predicting life (whether on the test stand or in the field). The energy associated with the change of phase from vapor back to liquid produces a significant pressure pulse that generates a resulting pressure wave in the fluid. This pressure wave interacts with the fluid and with the structure. If the pressure front is of a large enough level, the potential for erosion is high (depending upon the properties of the material).

Cavitation Noise Level

The connection between fluid noise and cavitation is well known. Researchers have long correlated increases in broadband fluid noise, typically in frequency bands greater than 20 kHz (Gopalakrishnan, 1985), with cavitation activity. Pearsall and McNulty (2004) showed that erosion damage in a special constriction tube (using high velocity to reduce pressure and form cavitation) increased with increase in fluid noise level.

Guelich (1989) further refined the use of fluid noise levels during tests with flow visualization. Guelich defined a measurement method that used a high-pass filter set at three-times blade pass frequency. This effectively eliminated signal content generated from fluid behavior that did not pertain to cavitation related activity, especially at reduced flow rates. The level of the remaining signal above a background level (established at a noncavitating suction pressure) was assumed dominated by cavitation activity. For the impellers evaluated by Guelich (1989) a good correlation was found between the peak noise level and the maximum erosion rate. He also tried to develop a calculation procedure to relate the measured noise level to cavitation erosion rates. However, for a field tool there are some limits to the use of this method:

- Placement of the sensor measuring the noise relative to the impeller
- Establishing a good noncavitating background level
- Difficulty dealing with cavitation noise at low flow rates where separation and recirculation can cause cavitation bubble collapse away from a surface limits the usefulness of this method.

From Guelich (1989), the noise level is found by calculating the rms level of the pressure signal, a (high-pass filtered above 3× blade pass), by Equation (3):

$$NL = \sqrt{\frac{n\sum a_i^2}{n}} \qquad (3)$$

The NL is normalized using the impeller inlet tip speed by Equation (4):

$$NL^* = NL \times \left(\frac{\rho U_e^2}{2g}\right)^{-1} \qquad (4)$$

Table of Contents

The noise level during noncavitating operation of the pump is referred to as NL_o*. This value provides the background noise level that would include the fluid noise at the specific flow rate of interest and any noise related to the transducer mounting but no cavitation noise. The difference between the measured level and the background level is referred to as the cavitation noise level and defined as Equation (5):

$$CNL^* = \sqrt{\left(NL^{*2} - NLo^{*2}\right)} \quad \textbf{(5)}$$

More recent efforts at developing cavitation detection methods were conducted in the hydraulic laboratory. The purpose of these efforts was to investigate noninvasive methods of detection and assessment of cavitation damage in pumps without relying on flow visualization or CFD analysis of two-phase behavior.

The test pump shown in Figure 2 is a full size model of a boiler feed pump suction stage. The model operated at reduced speed (1500 rpm), ambient temperature, and deaerated water. It is equipped with a complement of sensors described earlier. It provided a platform to investigate various signal acquisition and processing approaches for the purpose of characterizing the fluid and mechanical responses to cavitation activity.

Initial testing repeated the method of Guelich (1989) (Figure 8). Good correlation between the nondimensional cavitation noise level NL* and the dimensionless cavitation number, τ, was found. From field data, it was known that the suction impeller operated at a dimensionless cavitation number of 0.41 and had a very short cavitation life. This value for τ is very near the peak noise level for the 100 percent flow condition. The NL* plotted is not the CNL*. From Figure 8, at 100 percent flow the noise characteristic slope changes at a τ of about 1.5. The NL* value of .003 is the NLo*. Similarly at 50 percent flow the value is .004. This is an indication of where acoustic cavitation inception occurs and also the small difference in the filtered broadband noise level for these two flow rates. From flow visualization tests these values of τ are greater than where visual inception is perceived by the human eye.

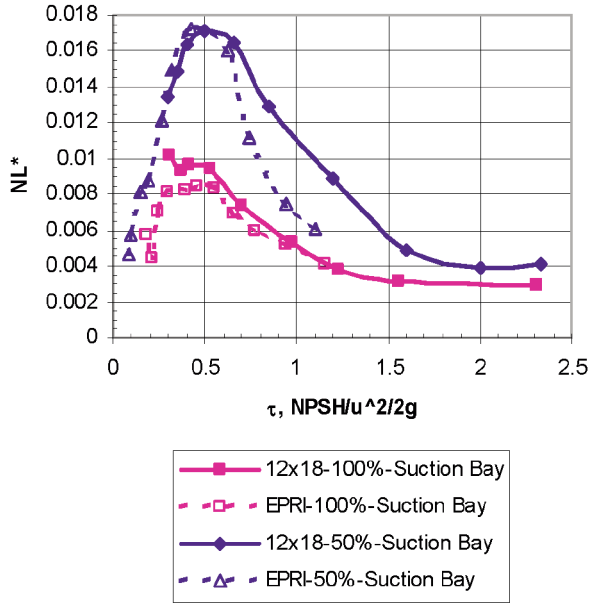

Figure 8. Cavitation Noise Level Measurements. (Fluid noise measurements on the test impeller shown in Figure 3 correlated well with Guelich test data. The peak noise level occurs at the NPSH level corresponding with plant operation.)

Replicating the work of Guelich (1989) in the field requires the installation of a pressure sensor through the pressure boundary of the pump or piping. The proximity of the sensor to the impeller is important in determining the measured noise level. The farther away, the more attenuated the level. The recent laboratory experience indicates that the best correlation with Guelich occurs when the pressure sensor is mounted inside the suction bay itself (often difficult to achieve when testing a barrel-type pump).

Being able to vary the NPSH across broad range is necessary in order to measure the background fluid noise level during noncavitating operation. This is sometimes difficult to do in the field. In fact, without the ability to generate a full mapping of the NL* versus cavitation number it would not be possible to identify the NPSH where peak damage level would occur.

For sheet type cavitation, the kind that is found when operating near the design flow (shown in Figure 1), relating the CNL* to a damage rate (which would require information regarding tip speed, system pressure, fluid conditions, etc.) may be possible. However, measuring the CNL* requires the complete NPSH mapping that includes noncavitating conditions. Also, at off-design flows, the noise level may not be indicative of the damage potential due to the collapse of bubbles away from the impeller surface. At off-design flow conditions suction recirculation from the impeller blades (a consequence of flow separation) destroys the sheet cavity and causes transport of some cavitation vapor to midstream, well away from a surface. However, some cavitation is also transported to the pressure side of the impeller blade or to the hub fillet, thus producing another area of damage. In summary, evaluating pumps in the field using this method is at best problematic and more likely impractical.

Fluid and Mechanical Response to Cavitation

The methodology of Guelich (1989) for calculating a CNL* can also be applied to other sensors mounted on or near the pump. Forces on bearings, casing and bearing housing vibrations, or airborne noise can be used to compare noise levels across the range of NPSH. Similar filtering can also be used. The power of filtering on eliminating noise level that is associated with noncavitating behavior can be seen when comparing signals from multiple sensors located on or near the test pump shown in Figure 2. The display in Figure 9 and 10 shows time waveforms of six different sensors that are very nearly in phase (only the settling time of a common analog to digital (A/D) converter causes any errors in phase, but this time shift is small in comparison to the total time of the sample). The types of sensors, shown from top to bottom of Figure 9, are:

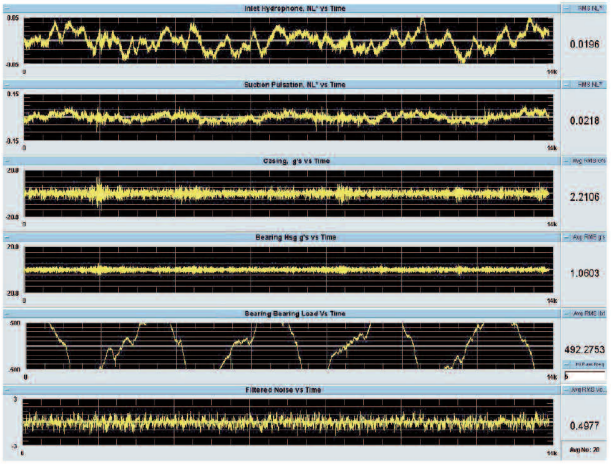

Figure 9. Unfiltered Time Waveforms (.75Q, .62τ). (Time waveforms measuring 0.2 seconds of operating data at 1350 rpm. These waveforms are obtained from the sensors shown on title bar. The all-pass frequency content includes all low frequency components.)

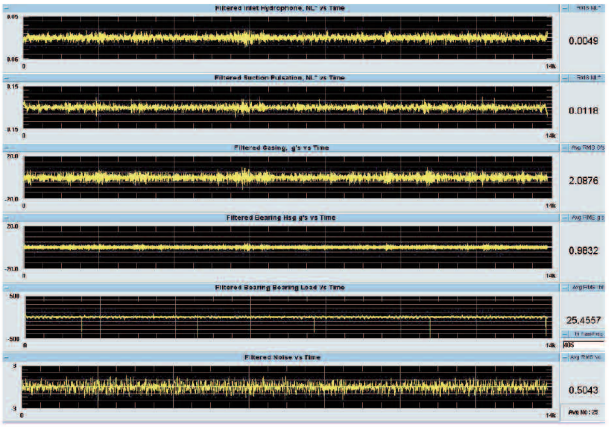

Figure 10. Digitally Filtered Time Waveforms (.75Q, .62τ). (Same acquisition time as Figure 9, but passing frequencies >3× blade pass. These filtered waveforms are used to calculate the rms values of each sensor per the Guelich [2000] method.)

- Inlet pipe mounted pressure transducer—NL*
- Suction inlet bay mounted pressure transducer—NL*
- Suction inlet bay mounted accelerometer—G's
- Bearing housing mounted accelerometer—G's
- Front radial bearing load cell (one direction)—lbf
- Airborne noise microphone in front of suction bay—volts proportional to decibels (dB) (conversion not known)

Each channel was digitized at approximately 70 kHz. The numerical values to the right of the waveforms are the rms levels calculated in the same manner as in Equation (2) (as described for NL). The set of waveforms in Figure 9 does not have the benefit of filtering. The waveforms in Figure 10 have been digitally filtered with an all pass filter set at >3× blade pass frequency. With the pump operating at 75 percent of design flow, there is some suction recirculation beginning. Impellers to diffuser blade interactions are also present. With the cavitation number set at $\tau = 0.62$, there are sheet cavity formations along with the onset of cavitation in the separated, recirculation zones in the impeller. Interpolating the curves from Figure 8, the peak NL* for this pump at 75 percent flow is about $\tau = 0.45$, so this NPSH is somewhat to the right of that value. While Figure 9 was acquired at a slightly different time than 10, the effect of the filtering is apparent. Of interest on Figure 10 is the appearance of multiple bursts of signal on top of the overall level. The amplitude of these bursts, above the continuum level, leads an observer to conclude that they are individual or overlapping implosions of large cavitation vapor volumes in the pump.

During the initial observation of this burst signal activity consideration was given to the idea that the burst activity was due to impacting of the impeller with the casing ring surface resulting in both fluidborne and structureborne impulse type signals. Bump testing of the rotor shaft and casing did not produce impulse activity of the type observed here. Also, the occurrence of the burst activity corresponded with the visual observation of cavity length growth and breakup in the cavity closure region.

Also apparent in Figure 10 is the common phase relationship between sensors for burst activity. In Figure 11, also 75 percent flow, but at a lower cavitation number, $\tau = 0.35$, a very rich period (0.2 seconds) of burst activity is observed on most of the sensors. Only the bearing load cell is apparently devoid of burst activity. This is possibly due to lack of sensitivity of the load cell that is configured to measure high loads and not low level fluctuations. Also seen on the bottom waveform is correlation of a burst of large amplitude and duration that is measured in the airborne noise signature. Amplitudes of the bursts seen in the fluid noise signatures can be five to 10 times the level of the NL* value. Similarly the vibration signals also show similar ratios of peak burst amplitude to the continuum level. Also the "ring-down" characteristic of the burst signature itself suggests that this is characteristic of a bubble collapse. In some instances there appears to be an observed "rebound" of the burst signal, also characteristic of a cavity implosion.

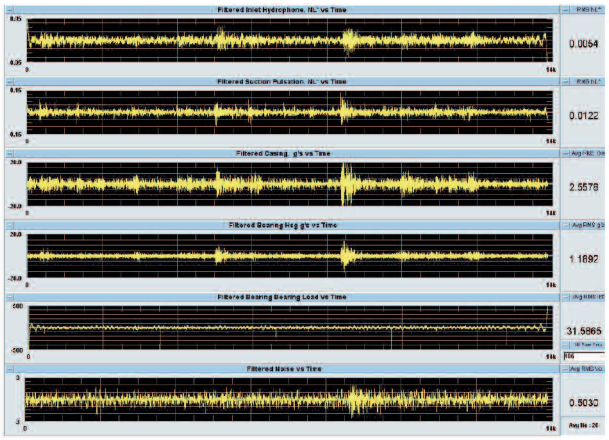

Figure 11. Unsteady Fluid/Structure Interaction at 75 Percent Flow, τ = 0.35. (These filtered time waveforms are shown in phase. These data cover 0.2 second of time or 4.5 shaft revolutions. One large event is observed that is measured on five of the six sensors. The numbers shown at the right of each waveform are the rms average value of the signal in the units called out in the title of each waveform plot.)

Testing over a range of flows and NPSH showed that the burst activity contributed significantly to the overall NL* value. It was also hypothesized that the burst activity was more indicative of cavitation damage than the overall increase in the continuum noise level that was observed during reduction of NPSH levels from noncavitating to fully cavitating conditions. These observations led to the development of a means to quantify the burst activity in an attempt to identify the extent to which the burst behavior is a better indicator of cavitation damage potential than the classic NL* characterization.

Quantifying Cavitation Burst Activity

The presence of signal bursts above the continuum noise was described by Gopalakrishnan (1985). A method of assessing the bursts was described then as spike above threshold (SAT). From Figure 11 it is easy to see the presence of such signals. Attempts to count burst activity above a threshold value for given flow and NPSH conditions were undertaken in this most recent work. This method required a setting of a threshold level, where a burst signal over this value indicates cavitation damage potential. Simple methods of counting the number of times the signal exceeded this threshold did not capture the characteristics of the high energy bursts in terms of amplitude and duration, both characteristics probably relevant to assess the energy available to cause erosion damage. This thinking led to the development of an enveloping scheme that could capture quantitatively what was visible and audible to an observer in terms of cavitation activity in the pump impeller.

The algorithm developed incorporated several mathematical operations applied to the signal sample that produced an envelope that modeled the signal as a series of bursts with amplitude and duration. An example of the enveloping process applied to a pressure sensor is shown in Figure 12. The top waveform shows a signal that has been filtered to pass signal with frequencies greater than 3× blade pass (the need to perform this filtering so that the bursts could be clearly identified was shown in Figure 11). Intermediate waveforms are shown and then the bottom waveform shows the envelope superimposed over the initial signal. Arrows are included to show how the bursts visible in the filtered signal are translated into an envelope.

Table of Contents

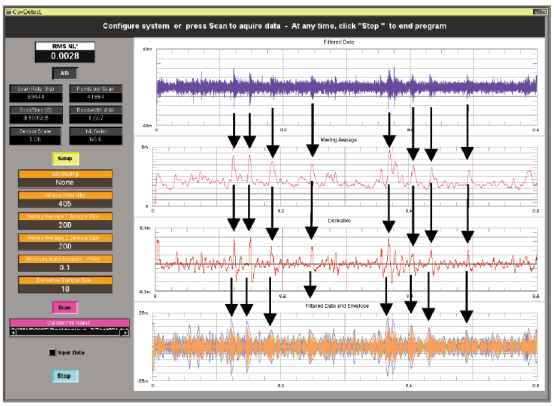

Figure 12. Screen Dump of Enveloped Hydrophone Signal Acquired During Cavitation. (The synthesized envelope is shown over the original filtered signal on the bottom trace. The simple enveloping algorithm converts cavitation bursts into a signal suitable for statistical evaluation and potential for damage.)

Burst events are identified in terms of level above a threshold amplitude and duration greater than a user-specified threshold limit. This threshold is usually related to the rms average signal level. Using specially developed software, burst events that fit the prescribed definition are cataloged.

Generating sets of burst data for different flow and NPSH conditions using identical sampling times is possible. Shown in Figure 13 is one approach. Samples of uniform time length were collected for a range of NPSH values at constant flow. For each NPSH condition, the signals were enveloped and bursts lasting over 3 milliseconds and having an NL* amplitude greater than 0.0204 were cataloged. Once those bursts were cataloged, the product of NL* and duration time in seconds were calculated for each burst. The burst-time products were grouped within ranges with the number of burst events occurring in each range plotted against cavitation number, using a three-dimensional contour plot. This approach to mapping is shown in Figure 13. For reference, to the left of the contour plot is the rmsNL* versus cavitation number, τ (a plot similar to Figure 8). The count of bursts in Figure 13 peaks between a τ-value of .040 to .035. This is identical to the rmsNL* level (a measure of the continuum level of the pressure signal). Further examination of burst activity at other flow rates indicated that the peak count of bursts coincided with the peak NL* levels calculated per Guelich's (1989) method.

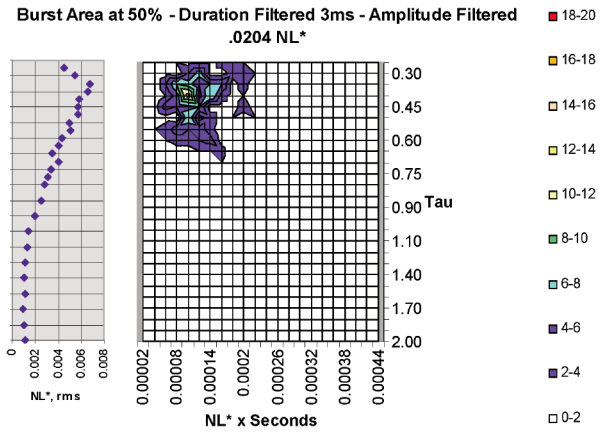

Figure 13. Contour Plots of Noise Intensity at 50 Percent Flow Rate. (The counts of bursts lasting longer than 3 milliseconds are plotted versus the area under the burst envelope (NL multiplied by time) plot and cavitation number, τ. The plot on the left hand side shows the rms NL* level versus τ. There is good correlation between the burst intensity and the peak NL* level.)*

Discussion of Detection Approaches

The test stand experience with the burst detection approach (or SAT) indicates that it offers no real improvement over the NL* measurement described by Guelich (1989). The burst method is more detailed in that the observer can see the increase in overall level of the signal with high amplitude bursts superimposed on the continuum level signal. The method can also be applied to casing or shaft vibration. However, the linkage between pressure levels that are normalized to tip speed (the NL* value) that make up the continuum and burst levels and the erosion potential of cavity collapse is tenuous due to the variability of the transfer function between the fluid and structural response for different pump configurations.

Common among all of the detection techniques discussed here is the question of how near to the impeller blade surface does the cavity collapse take place and how much of the energy is transferred to the surface. It is the accumulation of the energy of collapse on the surface of the blade that leads to material fatigue and in turn initiates and perpetuates the erosion process.

Further technology development is required to define a cavitation erosion potential assessment tool that meets the following criteria:

- Easily applied software algorithms using readily accessible instrumentation and software
- Straightforward and easily applied sensing elements
- Minimize reliance on transfer functions from fluid to mechanical response
- Reliable assessment conclusions

Significant progress has been made and demonstrated regarding improved impeller designs that provide acceptable levels of cavitation life. Also, progress is continuing on CFD based analysis of impellers that allow for optimization of designs for improved cavitation life across a wide flow range. However, until the state of computationally accurate predictions becomes common place (i.e., affordable and reliable), some form of tool will be required to judge pumps in the field and new designs on the test stand.

CONCLUSIONS AND RECOMMENDATIONS

Cavitation erosion in suction stage impellers increases life cycle costs in two major aspects. Costs of replacement and repair of a pump made inoperable by cavitation erosion is only one cost impact. The other is the reduction in pump availability and costs associated with process downtime. A significant amount of applied research and development has been conducted over the past several decades that addressed cavitation erosion in centrifugal pump impellers. Researchers have sought to characterize and quantify cavitation performance in terms of head drop, cavity length, erosion rate prediction, and acoustic or structural detection schemes. Much of this effort has improved impeller life and given insights into improved design approaches. Additionally, with the onset of multiphase CFD, reasonably accurate modeling of cavitation formation in impellers has been demonstrated.

However there still is a need for detection tools that can serve aftermarket concerns of pumps already in the field and that can also be applied to new design optimization efforts of manufacturers while on the test stand. The author suggests that future work addressing the detection and characterization of damage potential in pumps address the three criteria listed in the previous section.

- The availability of powerful and portable computer systems coupled with accurate and reliable signal acquisition hardware provides a wealth of high quality data to the engineer.
- However, the correct selection of sensors needed to feed the mechanical or fluid response to the system is necessary. These sensors must be practical, reasonably priced, and easily mounted or installed. This rules out mounting sensors directly on the impeller blades that are subject to damage.

- The need to eliminate mechanical interfaces between the surface of the impeller that is subject to damage and the point of sensing of the responses that indicate erosion potential is obvious. From the work reported on and referenced in this paper, it is observed that changes in cavitation level can me measured at many locations on the pump and piping. However there is one simple, more direct means of sensing cavitation that needs to be explored. This would be response of the shaft (with the impeller mounted either rigidly or loosely) to the multitude of cavitation implosions in close enough proximity to the shaft to cause erosion. Instrumentation does exist for shafts supported by antifriction bearings that detect bearing defects as measured by accelerometers on the bearing housing. For hydrodynamic bearings, shaft proximity measurements relative to the bearing housing serve to characterize the shaft reaction to various forces. Being able to sense a shaft response to the cavitation would seem to be the most direct means (short of placing sensors directly on the blade surface) of identifying cavitation behavior that causes erosion as opposed to cavitation behavior in the free stream that simply makes noise. A simple transfer function from the impeller through the shaft (a simpler shape than the prismatic configurations that constitute pump casings and suction inlets) is required to translate the vapor collapse energy to a mechanical response.
- Finally, the system should be reliable and avoid false negatives. False negatives lead to finding severe erosion in pumps with no prepared corrective plan in place.

While there are instrumentation packages that are tailored for or may be adapted to cavitation detection, it is incumbent upon the pump manufacturers to take the lead in interpreting the methods and algorithms. The tip speed and power level of the pump, range of operation, the fluid dynamics of off-design behavior, the physics of cavitation, the mechanical response of the impeller and shaft assembly, and the variability of pump installations requires the pump manufacturer to lead on such an effort.

Building on the work of those referenced in this paper will provide the tools needed to improve the reliability, performance, and operability of tomorrow's high-energy pumping machinery.

NOMENCLATURE

L_{cav}	= Cavity length
V	= Velocity
U	= Blade speed
g	= Acceleration due to gravity
NPSH	= Net positive suction head
NL*	= Normalized noise level
NLo*	= Normalized noncavitating noise level
CNL*	= Cavitation noise level
TS	= Tensile strength of material
F_{mat}	= Factor for type of material
A	= Liquid/gas properties factor
ρ	= Fluid density
ϕ	= Flow coefficient (V_m/U_e)
τ	= Cavitation number ($NPSH/Ue^2/2g$)

Subscripts

m	= Meridional component or mean
e	= Impeller inlet (eye) diameter

REFERENCES

Aisawa, T. and Schiavello, B., 1986, "Visual Study of Cavitation—An Engineering Tool to Improve Pump Reliability," *Proceedings of EPRI First International Conference on: Improved Coal-Fired Power Plants*, Palo Alto, California.

Bolleter, U., Schwarz, D., Carney, B., and Gordon, E., 1991, "Solution to Cavitation Induced Vibration Problems in Crude Oil Pipeline Pumps," *Proceedings of the Eighth International Pump Users Symposium*, Turbomachinery Laboratory, Texas A&M University, College Station, Texas, pp. 21-28.

Cooper, P., 2000, "Centrifugal Pump Theory," Section 2.1 of the *Pump Handbook*, Third Edition, New York, New York: McGraw-Hill.

Cooper, P. and Antunes, F. F., 1982, "Cavitation in Boiler Feed Pumps," *Symposium Proceedings on: Power Plant Feed Pumps-The State of Art*, EPRI CS-3158, Cherry Hill, New Jersey.

Cooper, P., Sloteman, D. P., and Graf, E., 1991a, "Design of High-Energy Impellers to Avoid Cavitation Instabilities and Damage," *Proceedings of EPRI Symposium on: Power Plant Pumps*, Tampa, Florida.

Cooper, P., Sloteman, D. P., Graf, E., and Vlaming, D. J., 1991b, "Elimination of Cavitation-Related Instabilities and Damage in High-Energy Pump Impellers," *Proceedings of the Eighth International Pump Users Symposium*, Turbomachinery Laboratory, Texas A&M University, College Station, Texas, pp. 1-20.

Dernedde, R. and Stech, P. R., 1982, "Design of Feed Pump Hydraulic Components," *Symposium Proceedings on: Power Plant Feed Pumps—The State of the Art*, EPRI CS-3158, Cherry Hill, New Jersey.

Florjancic, D., 1980, *Mindestzulaufhoehen fuer speisepumpen (Minimum Suction Conditions for Feed Water Pumps)*, VGB, Kraftwerkstechnik 60, Heft 12.

Gopalakrishnan, S., 1985, "Modern Cavitation Criteria for Centrifugal Pumps," *Proceedings of the Second International Pump Symposium*, Turbomachinery Laboratory, Texas A&M University, College Station, Texas, pp. 3-10.

Guelich, J. F., 1989, *Guidelines for Prevention of Cavitation in Centrifugal Feed Pumps*, EPRI GS-6398.

Hergt, P., Niklas, A., Moellenkopf, G., and Brodersen, S., 1996, "The Suction Performance of Centrifugal Pumps Possibilities and Limits of Improvements," *Proceedings of the Thirteenth International Pump Users Symposium*, Turbomachinery Laboratory, Texas A&M University, College Station, Texas, pp. 13-26.

Makay, E. and Szamody, O. 1978, "Survey of Feed Pump Outages," EPRI Report FP-754.

Pearsall, I. S. and McNulty, P. J., 2004, "Comparison of Cavitation Noise with Erosion," National Engineering Laboratory, East Kilbride, Glasgow, United Kingdom.

Rayleigh, L., 1917, "On the Pressure Developed in a Liquid During the Collapse of a Spherical Cavity," *Philosophical Magazine*, Series 4, (34), pp. 94-98.

Schiavello, B. and Prescott, M., 1991, "Field Cases Due to Various Cavitation Damage Mechanisms: Analysis and Solutions," *Proceedings of EPRI Symposium on: Power Plant Pumps*, Tampa, Florida.

Sloteman, D. P., Robertson, D. A. ,and Margolin, L., 2004, "Demonstration of Cavitation Life Extension for Suction-Stage Impellers in High Energy Pumps," *Proceedings of the Twenty-First International Pump Users Symposium*, Turbomachinery Laboratory, Texas A&M University, College Station, Texas, pp. 103-115.

Sloteman, D. P., Wotring, T. L., March, P., McBee, D., and Moody, L., (1995), "Experimental Evaluation of High Energy Pump Improvements Including Effects of Upstream Piping," *Proceedings of the Twelfth International Pump Users Symposium*, Turbomachinery Laboratory, Texas A&M University, College Station, Texas, pp. 97-112.

Thiruvengadam, A., 1973, "Handbook of Cavitation Erosion," Hydronautice, Incorporated, Technical Report 73-1-1 Office of Naval Research, Department of the Navy, AD-787-073.

Vlaming, D. J., July 1989, "Optimum Impeller Inlet Geometry for Minimum NPSH Requirements for Centrifugal Pumps," *Pumping Machinery*, ASME, pp. 25-29.

ACKNOWLEDGEMENTS

The author wishes to thank his management at Curtiss-Wright, Engineered Pump Division for permission to write this paper and to Mr. Timothy Wotring, Vice President, Engineering of the Flowserve Pump Division for allowing him to use the test data and program results acquired with their test equipment and technical support. Special thanks go to the late Dr. S. Gopalakrishanan, Vice President, Technology of the Flowserve Pump Division for sponsoring and supporting the detection and assessment work described in this paper. Some of the material included in this paper was presented at a special ASME session in 2006 honoring the career of Dr. Gopalakrishnan. Dr. Paul Cooper organized this session. Individuals who supported the work described here include Mr. Leo Margolin, Mr. Kim Horten and Mr. Mathew Nothnagel of Curtiss-Wright, Engineered Pump Division. Mr. Bruno Schiavello of Flowserve Pump Division supported and contributed to the content of this work.